Mineralogical Magazine, August 2002, Vol. 66(4), pp. 491–512

Structural states of micas in amphibolites of the KSDB-3 deep bore-hole and their surface equivalents

N. O. Ovchinnikov[1,*], L. P. Nikitina[1], M. S. Babushkina[1], A. K. Yakovleva[2], Yu. N. Yakovlev[2], O. G. Chernova[3] and S. A. T. Redfern[4]

[1] Institute of Precambrian Geology and Geochronology, Russian Academy of Science, Makarova emb. 2, St. Petersburg, 199034, Russia
[2] Scientific Industrial Centre 'Kola Superdeep', Zapolyarny, Murmansk region, 184415, Russia
[3] Mineralogy Department, St. Petersburg State University, Universitetshaya emb. 7/9, St. Petersburg, 199034, Russia
[4] Department of Earth Sciences, University of Cambridge, Downing Street, Cambridge CB2 3EQ, UK

ABSTRACT

Trioctahedral ferromagnesium micas from the Archaean amphibolites of the Kola super-deep borehole (KSDB-3) complex have been compared with those from analogous Archaean surface rocks in an integrated study of their chemical compositions and structural states (using wet chemistry, microprobe, X-ray, Mössbauer and infrared methods). Reports on both the experimental procedure and the crystal chemistry of the trioctahedral micas are given. This has enabled the revision of the assignment of individual infrared (IR) absorption bands for the hydroxyl ion (ν_{OH^-}), and demonstrated the possibility of determining the content of Mg, Fe^{2+}, R^{3+} cations and vacancies in the octahedral sheet to within a few hundredths of atomic units on the basis of the infrared and Mössbauer data. Proof was found of the presence of molecular water replacing K^+ in the interlayer, which results in anomalous variations in the cell parameters, as the mica structure expands in response to the ingress of H_2O. Variations in the degree of non-stoichiometry of the micas is related to the presence of structural H_2O and of octahedral *M*1 vacancies. We found that samples recovered from depth within the borehole display lower degrees of octahedral order than those found in the analogous surface rocks.

Keywords: phlogopite, biotite, infrared, Mössbauer, crystal structure, order-disorder, defect chemistry.

Introduction

The Kola super-deep borehole (KSDB-3) is situated in the northeastern part of Baltic shield within the Pechenga Block. It intersects Precambrian rocks down to a depth of 12262 m and provides a unique opportunity to study the dependence of physical and chemical properties of rocks and minerals on depth within the Earth's crust. Such investigations may illuminate models of the crust as a whole and enhance our understanding of geophysical data as well as the processes of the concentration and mass-transfer of material within the crust.

Bearing in mind what is known of the thermodynamics and kinetics of order-disorder transformations in rock-forming minerals (e.g. Virgo and Hafner, 1969; Khristoforov *et al*., 1974; Saxena *et al*., 1987; Skogby, 1987; Babushkina, 1993; Pavese *et al*., 2000; Bosenick *et al*., 2001), we may assume that the minerals from the Archaean complex of KSDB-3 (from depths of 6842 to 12262 m) were quenched as a result of rapid exhumation from great depth to the surface during bore-hole drilling. In this case, their structural states preserve the deep equilibrium conditions in the Earth's crust (Nikitina and Yakovleva, 1999). In contrast, the Archaean rocks at the erosion surface (the analogues on the surface) were elevated slowly and had the opportunity to re-equilibrate on slow exhumation at changing temperatures and pressures. Thus we anticipate differences in the structural state of the

* E-mail: nikita@ad.iggp.ras.spb.ru
DOI: 10.1180/0026461026640044

minerals from the rocks of Archaean deep borehole section and their surface equivalents. In particular, differences in the details of their defect structures may be especially important, as these depend most sensitively on temperature and pressure. These may be apparent as differences in the mixing limits of solid solutions, the degree of cation ordering, iron oxidation state (as well as that of other polyvalent cations), the occurrence of defect water (hydroxyl, and other defect hydrous complexes) and other volatiles, as well as differences in the degree of non-stoichiometry of the phases present.

The details of these structural features may provide an explanation as to why some rocks recovered from great depth in the Archaean complex, which consists mainly of acidic rocks (gneisses and granitoids), show densities and elastic wave velocities more characteristic of mafic rocks. Early geophysical observations were therefore interpreted in terms of the presence of a basalt layer at depths of >7−7.5 km, although this has not been found by subsequent drilling (Lanev *et al*., 1984).

In previous studies (Nalivkina *et al*., 1984; Nalivkina and Vinogradova, 1986; Yakovleva, 1991), the compositions of the rock-forming minerals (principally amphibole, biotite, clinopyroxene, plagioclase) and ore minerals were determined in detail and trends in the changes of mineral compositions and structural states in the Proterozoic and Archaean complexes of the borehole were established. As a first step, the dependencies of Al/Si order-disorder in plagioclase and the amount of Fe^{2+} in amphiboles on depth were established. However, these investigations can only be considered preliminary. The application of modern physical, chemical and structural methods is needed to study the detailed structural state of minerals from the borehole section of the Archaean complex, as well as their surface counterparts.

As a first step we have studied the structure of rock-forming Fe-Mg bearing minerals (micas and amphiboles) in mafic and ultramafic rocks, from both the Archaean complex at depths between 7926.0 and 11334.2 m as well as their surface counterparts. Amphibolites make up ~34% of this portion of the Archaean complex. These amphibolites, represented by numerous small bodies 0.5−1.0 to 20−30 m thick (rarely more), have intersecting and concordant contacts with gneisses (Nalivkina *et al*., 1984; Yakovleva *et al*., 1991; Yakovlev and Yakovleva, 2000).

The amphibolite-gneiss complex at the southern edge of the Pechenga structure (the Allarechka block) is believed to be the counterpart of the KSDB-3 Archaean complex. A comparison of the Archaean rocks of KSDB-3 and the Allarechka amphibolite-gneiss complex was carried out by comparing their overall features, the most significant of which are their ages and the geodynamic conditions of their formation. This comparison confirms that the amphibolite-gneiss at the surface and the samples from the borehole are indeed similar, with like chemical and mineralogical compositions.

The Archaean amphibolite-gneiss complex of the Allarechka region contains several gneisses (biotite, amphibole-biotite, garnet-biotite, two-mica), amphibolites, massive granitoids as well as ultramafic bodies with industrial copper-nickel mineralization (Yakovlev and Yakovleva, 1974; Zagorodniy and Radchenko, 1978, and others). The complex was metamorphosed to amphibolite facies, granitized and crossed by granite pegmatite veins. At the contact of these veins and the ultramafic bodies (and rarely the amphibolites) reaction rims are formed (Yakovlev and Yakovleva, 1974). The rocks of the amphibolite-gneiss complex of the Allarechka ore field are similar to the rocks in this interval of the KSDB-3 section, including the 'II−VIII' formation (7600−11400 m; Smirnov *et al*., 1991).

In the present paper, the results of a comprehensive study of the compositions and structures of the micas are reported. The results of an analogous study of amphiboles will be reported in a further paper.

Crystal structure of trioctahedral micas

The structural details and crystal chemistry of micas are reported elsewhere (e.g. Tischendorf *et al*., 2001). Importantly for this study, it is worth re-emphasizing that there are two types of octahedral sites in the mica structure, which differ in OH^- position, symmetry and dimensions. In the *M*1 octahedron (C_{2h}) OH^- anions are in *trans* orientation, at the *M*2 (C_2) they are in *cis* orientation. The ratio of *trans* (*M*1) to *cis* (*M*2) octahedra is 1:2. The connection of octahedra into layers occurs along edges, formed by O^{2-} and OH^- anions, in such a way that each *M*1 octahedron has six common edges with six *M*2 octahedra. Each *M*2 octahedron also has six nearest neighbour octahedra within the sheet, but half of them are of *M*1 type and the other half

are *M*2. Each cation in *M*1 is thus surrounded by six cations in *M*2 ($n_2^{M1} = 6$; $n_1^{M1} = 0$), while each cation in *M*2 is surrounded by three cations in *M*1 ($n_1^{M2} = 3$) and by three in *M*2 ($n_2^{M2} = 3$).

Isovalent ($Mg^{2+} \rightarrow Fe^{2+}$) and heterovalent ($Mg^{2+}$, $Fe^{2+} \rightarrow Al^{3+}$, Fe^{3+}, Ti^{3+}) substitutions in the octahedral sheet are possible. Mössbauer and IR studies of micas, annealed at 500–650°C in evacuated (0.01 Pa) quartz tubes for periods of up to 240 h, indicate that the octahedral Ti may be trivalent (Babushkina *et al*., 1997). At these conditions, the OH^- anions, coordinated by two cations and a vacancy are partly driven off (the intensity of V bands decreases), but oxidation of Fe^{2+} does not occur, according to the Mössbauer data. This means that there has to be a cation, such as Ti^{3+}, present in the octahedral sheet which can become more oxidized. This conclusion is in accordance with photoelectron X-ray data for natural phlogopites and biotites (Evans and Raftery, 1980), and with electron paramagnetic resonance (EPR) and optic absorbtion data for synthetic fluorphlogopites (Matveev *et al*., 1981). These data have been interpreted such that Ti cations mainly occupy octahedral sites in a trivalent state. However, we note that while Lalonde and Bernard (1993) inferred Ti^{3+} in biotite on the basis of colouration, Henderson and Foland (1996) found little evidence for Ti^{3+} in a high-Ti mica.

Isovalent substitution is prevalent and leads to the formation of solid solutions of the phlogopite–annite series. Heterovalent substitutions in a 1:1 ratio must be charge compensated by $Si^{4+} \rightarrow Al^{3+}$ substitution on the tetrahedral sublattice. The tetrahedral Al content in natural micas may reach 1.5 atoms per formula unit (a.p.f.u.). A heterovalent replacement according to the scheme $3R^{2+} \rightarrow 2R^{3+} + V$ may also take place (Osherovitch *et al*., 1975; Sanz *et al*., 1984; Babushkina *et al*., 1989; Ponomarev and Lapides, 1990). Micas with non-stoichiometric compositions and large concentrations of octahedral vacancies are very common in lamproites (Babushkina *et al*., 1997, 2000).

X-ray crystal structure refinement of trioctahedral micas (Bailey, 1984), tends to indicate that tetrahedral Si^{4+}, Al and Fe^{3+} are disordered. Following the Radoslovich rule, the trivalent cations are believed to occupy the *M*2 sites (Radoslovich, 1963). In tetra-ferriphlogopites and tetra-ferribiotites, Fe^{3+} occupies the octahedra and/or tetrahedra, as shown by X-ray studies (Semenova *et al*., 1977; 1983; Pavlishin *et al*., 1978; Cruciani and Zanazzi, 1994), Mössbauer spectroscopy (Annersten *et al*., 1971; Dyar, 1987; Rancourt *et al*., 1992; Cruciani *et al*., 1995; Babushkina *et al*., 1997, 2000) and, also, by nuclear magnetic resonance (NMR) and XANES spectroscopy methods. In low-aluminous micas from lamproites there may be a deficiency in Si and Al in the tetrahedral sites, which can be made up by Fe^{3+}, as well as by Ti, even if the total Fe^{3+} content is more than the total of tetrahedral vacancies (Babushkina *et al*., 1997, 2000). The Ti_{IV}/Fe^{3+}_{IV} ratio may vary within wide limits (being more or less than unity). In micas from lamproites, $Fe^{3+}_{IV}/Fe^{3+}_{VI}$ ratios from 0.6 to 2.3 have been reported, and the preference of Fe^{3+} occupation of tetrahedral or octahedral sites cannot be stated confidently.

The distribution of divalent cations between nonequivalent octahedral sites suggested by structure refinements of phlogopite, tetra-ferriphlogopite, tetra-ferribiotite (Semenova *et al*., 1977; 1983) as well as synthetic (Drits *et al*., 1971) and natural biotites (Takeda and Ross, 1975; Bohlen *et al*., 1980) and oxibiotites (Ohta *et al*., 1982) is disordered or only weakly ordered. However, Mössbauer spectroscopy reveals long-range ordering of Fe^{2+} between the *M*1 and *M*2 sites (Bancroft and Brown, 1975; Osherovitch *et al*., 1978; Babushkina and Nikitina, 1985; Babushkina, 1993; Dyar and Burns, 1986; Ivanitzky *et al*., 1992; Babushkina *et al*., 1989, 1997, 2000). The application of NMR and IR spectroscopy allows one to establish the type of short-range order of cations in the octahedral sheet. In the structure of OH^- and F-bearing biotites, the OH^- anions are surrounded predominantly by Fe cations and F^- anions by Mg cations (Sanz *et al*., 1978; Sanz and Stone, 1979, 1983). The preferential formation of the mixed triplet groups MgMgFe, FeFeMg, MgFe*R* (*R* = trivalent cation) and asymmetric pair groups Mg-Fe, Mg-*R*, Fe-*R* in the octahedral sheet has been established in numerous studies (e.g. Osherovitch and Nikitina, 1975; Babushkina *et al*., 1989, 1997, 2000).

In natural micas water may be present not only as OH^- anions, but also in other forms. The presence of H_2O molecules, which are connected to the structure by hydrogen bonds, is suggested by broad IR absorption bands in the 3500–3000 cm^{-1} region (corresponding to the stretching vibrations of molecular water, ν_{H_2O}) and from 1650 to 1630 cm^{-1} (water bending vibrations, δ_{H_2O}). In the IR spectra of micas from

lamproites several absorption bands in these regions were observed and their integral intensity inversely correlated with the occupancy of K^+ in the interlayer site (Babushkina *et al*., 1997, 2000). On this basis, it is supposed that H_2O molecules occupy the interlayer cavities, as suggested in relation to white micas by Loucks (1991).

Experimental methods

The compositions of micas were determined by wet chemistry at the Kola Geological Institute RAS, as well as by electron microprobe analysis (LINK AN 1000 electron microprobe with an accelerating voltage of 15 kV, current strength of 0.4−0.5 mA and 2−5 μm beam diameter) at the Institute of Precambrian Geology and Geochronology, RAS. The Fe_2O_3 and FeO contents were determined by Mössbauer spectroscopy. The crystal structures, as well as the character and degree of structural defects were studied by X-ray powder diffraction at St. Petersburg State University (Geological Department) and by Mössbauer and IR spectroscopy at the Institute of Precambrian Geology and Geochronology RAS.

X-ray powder diffraction also provided a check on the sample purity, polytype modification and unit-cell parameters. X-ray data were recorded on a DRON-2.0 diffractometer using graphite monochromated Co-K_α radiation. Least-squares refinement of the 002, 200, 201, 202, 005, $13\bar{5}$, 060, 007, $20\bar{7}$ and 008 reflections gave the lattice parameters.

The Fe^{3+}/Fe^{2+} ratio and their distributions were obtained by Mössbauer spectroscopy. The Mössbauer spectra were recorded on an SMB-2201 spectrometer with a constant acceleration electrodynamic velocity generator and a 30 mCurie ^{57}Co in Cr source. The spectra were recorded at room temperature in the velocity interval from +5 to −5 mm/s. In order to eliminate the asymmetry of quadrupole doublets, due to preferred orientation of mica grains, the absorber was mixed with polyethylene and then was pressed as a cone. The angle between the normal to the generatrix of the cone and the γ radiation direction was set to 54.7°. The density of natural Fe in the absorber was 5 mg/cm^3. The spectrometer was calibrated using natural Fe foil. The Mössbauer spectra were fitted to pure Lorentzian lines. Computer fits were evaluated by χ^2 and MISFIT. Ideally, χ^2 divided into the number of degrees of freedom should approach the 1.00, and MISFIT should be zero for a perfect fit. In our case their values were: $0.99 < \chi^2 < 1.10$ and $0.004 <$ MISFIT < 0.050. Peak areas and half-widths (HW) for each doublet were constrained to remain equal.

The Mössbauer spectra of our micas were fitted using three or four doublets. The doublet with isomer shift (IS) 0.44/0.65 mm s^{-1} and quadrupole splitting (QS) 0.48/1.28 mm s^{-1} was assigned as Fe^{3+} in octahedral coordination, the doublet with IS = 0.08 mm s^{-1} and QS = 0.66mm s^{-1} was assigned as Fe^{3+} in tetrahedral coordination. The doublets with 1.12 mm s^{-1} < IS < 1.25 mm s^{-1} and QS > 2.2 mm s^{-1} were assigned as Fe^{2+} in octahedral sites. The results of theoretical simulations of biotite spectra based on point charge models (Mineeva, 1978) and experimental spectra of micas with Fe^{2+} contents of 0.2−2.20 a.u. at 298 and 77 K were used for the assignment of Fe^{2+} in *M*1 and *M*2 octahedra based on these doublets (Osherovich *et al*., 1978). The experimental data show a strong QS temperature-dependence and amount of Fe assigned to the outer doublet in the high-temperature spectra and to the inner doublet in the low-temperature spectra changes by a factor of nearly two. In spectra of Fe-bearing micas it greatly exceeds 1.0 a.u. Therefore in spectra recorded at 298 K the outer doublet (2.58 mm s^{-1} < QS < 2.75 mm s^{-1}) was assigned to Fe^{2+} in the *M*2 site and the inner one (2.21 mm s^{-1} < QS < 2.48 mm s^{-1}) to Fe^{2+} in *M*1 site. The assignment in low-temperature spectra is opposite. Our assignments are in agreement with those reported previously (e.g. Dyar, 1984, 1987; Ivanitsky *et al*., 1992; Cruciani *et al*., 1995). The relative amounts of Fe^{2+} and Fe^{3+} and the occupancy of Fe in each site have thus been calculated from the integral intensity ratio of the appropriate doublets. The recoil-free fractions for ferric and ferrous Fe are equal to 1.0 in non-equivalent sites. The error in the Mössbauer spectra parameters is ±0.009 mm s^{-1}, which translates to an error in the determination of the proportions of ferrous and ferric Fe in non-equivalent sites of ±1%.

Hydrous species and the nature of short-range cation order in the octahedral sheet were studied by IR spectroscopy using a Specord M80 double-beam diffraction grating spectrophotometer operating from 3800 to 3000 and 1750 to 1400 cm^{-1} with a resolution of 0.5 cm^{-1} and a dry air purge. The fine-dispersed samples were milled in an agate vial under acetone then sieved to a grain-size of 3−10 μm. The lack of Fe oxidation during

grinding was checked more than once by comparison of Mössbauer spectra of milled and unmilled samples. The powdered samples were annealed at 300°C for 3 h in evacuated (<0.01 Pa) quartz ampules and then quenched in liquid nitrogen, to remove unbound water. Then, 20 mg of sample were diluted in 500 mg of dry KBr and pressed as a pellet at a vacuum pressure of 1 Pa and a temperature of 100°C. This method of pellet preparation avoided the presence of the absorption bands due to non-structural water in the region 3500−3000 cm^{-1}. Absorption bands in this region may still arise, however, from structural H_2O.

The IR spectra were fitted using mixed Lorentzian-Gaussian profiles. All spectral parameters were varied. Due to our method of pellet preparation, the baseline of low- and high-frequency absorption edges lay practically on the same line, reducing the error in determination of integral intensity of the OH^- (ν_{OH^-}) stretching modes. Computer fits were evaluated by the discrepancy of the fit and by the degree of concordance of octahedral occupation by cations obtained by IR, microprobe, wet chemistry and Mössbauer spectroscopy.

The assignment of stretching vibration bands of OH^- anions, coordinated with triple groups of divalent cations (N-bands), of di- and trivalent cations (I-bands), of di-trivalent cations and vacancies (V-bands) was carried out according to Vedder (1964) with further revision by Wilkins (1967), Farmer *et al.* (1971), Rausell-Colom *et al.* (1971), Rousseaux *et al.* (1972), Sanz *et al.* (1983), Babushkina *et al.* (1997). We also bore in mind that some cation combinations, which are possible in theory, are forbidden or low-probability according to crystal chemical considerations (Radoslovich, 1963; Pauling, 1960). More details concerning the assignment of individual absorption bands into N, I and V groups are discussed below.

Results

The geological locations of our micas are shown in Table 1. Here, and elsewhere, the micas from depths of 10−247 m are considered as surface analogues. The chemical compositions of these micas are given in Table 2. On the diagram $(MgO+FeO)$-Al_2O_3-SiO_2 (Fig. 1) these compositions lie along the line of the stoichiometric compositions of iron-magnesia trioctahedral

TABLE 1. Geological positions of the samples.

Sample	Mineral	Rock	Depth, m
Archaean complex in the section of KSDB-3			
26524	Phlogopite	Phlogopite-anthophyllite-actinolite amphibolite	7896.8
26633	Phlogopite	Phlogopite-anthophyllite-actinolite amphibolite	7926.0
28248-g	Phlogopite	Phlogopite-anthophyllite-actinolite amphibolite	8428.9
35899-2	Phlogopite	Phlogopite-anthophyllite-actinolite amphibolite	9670.0
35967-4	Phlogopite	Phlogopite-anthophyllite-actinolite amphibolite	9675.2
37483	Biotite	Biotite amphibolite	10100.3
43452	Biotite	Garnet-clinopyroxene amphibolite	11334.2
27053	Biotite	cummingtonite-hornblende amphibolite	7964.7
42749-2	Biotite	Cummingtonite-hornblende amphibolite	10171.8
Analogues at the surface (Allarechensky region)			
99/46.4	Phlogopite	Metaperidotite with Cu-Ni ore	46.4
1394/45.0	Phlogopite	Metaolivinite	45.0
410/135.0	Phlogopite	Phlogopite-anthophyllite-actinolite rock (reaction zone in metaolivinite)	135.0
410/225.0	Phlogopite	Phlogopite-anthophyllite-actinolite rock (reaction zone in metaolivinite)	225.0
1394/45.0	Phlogopite	Phlogopite-anthophyllite-actinolite amphibolite (metaolivinite)	45.0
130/40.7	Biotite	Phlogopite-anthophyllite-actinolite amphibolite (metaperidotite)	40.7
247/246.9	Biotite	Biotite-hornblende rock on the contact with ultramafic rock	246.9
9,10	Biotite	Biotite plagioclase-amphibolite	0.0
2757/71.0	Biotite	Garnet-clinopyroxene amphibolite	71.0

TABLE 2. Composition of the micas.

Oxide	265246 1	26633 2	27053 3	28248-g 4	35899-2 5	35967-4 6	37483 7	42749-2 8	43452 9
KSDB-3									
SiO_2	41.42	42.49	39.96	37.74	42.10	40.50	38.16	39.16	37.98
TiO_2	0.93	0.68	1.56	0.04	0.62	0.80	1.74	1.02	2.05
Al_2O_3	12.92	14.45	15.99	18.35	13.54	15.84	15.63	17.63	14.46
Cr_2O_3	0.47	0.00	0.00	0.13	0.70	0.64	0.28	0.05	0.26
Fe_2O_3	1.42	0.00	1.24	0.99	2.38	0.70	1.22	0.54	1.86
FeO	11.58	7.18	12.52	7.42	6.64	7.24	13.08	12.97	15.54
MnO	0.09	0.00	0.04	0.04	0.05	0.02	0.04	0.06	0.08
MgO	17.02	22.48	15.37	20.31	21.30	20.23	15.47	15.08	13.79
CaO	0.20	0.00	0.00	0.00	0.52	0.06	0.20	0.39	0.61
Na_2O	0.09	0.36	0.20	0.31	0.52	0.42	0.29	0.33	0.28
K_2O	8.97	8.72	9.04	8.25	7.35	8.38	8.57	8.39	9.09
NiO	0.00	0.00	0.00	0.04	0.18	0.25	0.15	0.08	0.00
H_2O^+	3.65	n.d.	n.d.	4.54	3.66	4.17	3.97	3.93	3.15
F^-	0.75	n.d.	n.d	0.18	0.23	0.14	0.21	0.07	0.27
Σ	98.76	96.36	95.92	98.34	99.79	99.39	99.01	99.70	99.12
fm	0.30	0.15	0.33	0.18	0.19	0.18	0.34	0.33	0.41
Crystal chemical coefficients									
Si	3.03	2.98	2.90	2.74	2.97	2.89	2.83	2.85	2.84
Al_{IV}	0.97	1.00	1.03	1.26	1.03	1.11	1.17	1.15	1.16
Fe^{3+}_{IV}	0.00	0.00	0.07	0.00	0.00	0.00	0.00	0.00	0.00
Σ_{IV}	4.00	4.00	4.00	4.00	4.00	4.00	4.00	4.00	4.00
Ti	0.05	0.04	0.08	0.00	0.03	0.04	0.10	0.06	0.12
Al_{VI}	0.14	0.17	0.34	0.32	0.10	0.23	0.20	0.36	0.11
Cr	0.03	0.00	0.00	0.01	0.04	0.04	0.02	0.00	0.02
Fe^{3+}	0.08	0.00	0.00	0.05	0.13	0.04	0.07	0.03	0.11
Fe^{2+}	0.71	0.42	0.76	0.45	0.39	0.43	0.81	0.79	0.97
Mn	0.01	0.00	0.00	0.00	0.00	0.00	0.00	0.00	0.00
Mg	1.85	2.35	1.66	2.2	2.24	2.15	1.71	1.64	1.53
Ni	0.00	0.00	0.00	0.00	0.01	0.01	0.01	0.00	0.00
Σ_{VI}	2.86	2.98	2.84	3.03	2.93	2.94	2.92	2.88	2.86
Ca	0.02	0.00	0.00	0.00	0.04	0.00	0.02	0.03	0.05
Na	0.01	0.05	0.03	0.04	0.07	0.06	0.04	0.05	0.04
K	0.84	0.78	0.84	0.76	0.66	0.76	0.81	0.78	0.87
Σ_{XII}	0.87	0.83	0.87	0.80	0.77	0.82	0.87	0.86	0.96
Charge IV+VI	21.07	21.09	21.0	21.18	21.15	21.07	21.06	21.06	20.92

micas. At the same time the micas from the bore-hole deviate from this line, being deficient in MgO + FeO compared with the surface micas. Moreover the total charge per formula unit of octahedral and tetrahedral cations of micas from the bore-hole is more than +21, while this charge for some surface micas is lower than or equal to +21.

The unit-cell parameters of phlogopites and biotites are given in Table 3. The dependence of unit-cell parameter *c* and volume *V* on *fm* {*fm* = $(Fe^{2+} + Fe^{3+})/(Fe^{2+} + Fe^{3+} + Mg)$} is given in Fig. 2. Included in this figure are corresponding values for end-members of the synthetic phlogopite-annite series (Bailey, 1984) and of comparable micas (with Fe^{3+} <0.13 and Al_{VI} <0.35 a.u.) from metamorphic and igneous rocks from other regions. In Fig. 2*a*, the data for micas from SKDB-3 and its surface analogues form two different trends, which reflect the decrease of *c* parameter with increasing *fm*, in contrast to the positive dependence of *c* for the synthetic phlogopite–annite series. In the plot of *V vs. fm* (Fig. 2*b*), the points for all micas lie in general along the line connecting the end-members of the

TABLE 2 (*continued*)

Oxide	410/135.0 10	410/225.0 11	1394/45.0 12	130/40.7 13	99/46.4 14	247/246.9 15	9,10 16	2757/71.0 17
Surface								
SiO_2	40.77	38.75	38.99	36.58	40.31	37.20	34.89	36.82
TiO_2	0.51	0.87	0.93	1.90	0.73	2.87	2.87	2.64
Al_2O_3	13.94	13.29	14.31	15.43	14.12	14.53	16.71	15.13
Cr_2O_3	0.47	0.44	0.47	0.00	0.00	0.00	0.00	0.07
Fe_2O_3	1.14	3.25	1.72	0.92	1.59	0.74	1.45	2.73
FeO	7.45	7.90	8.52	17.83	5.35	17.39	21.92	17.87
MnO	0.03	0.06	0.03	0.11	0.00	0.10	0.23	0.21
MgO	21.72	21.37	21.34	13.14	23.83	14.32	8.31	10.50
CaO	0.14	0.14	0.00	0.17	0.00	0.12	0.86	0.18
Na_2O	0.25	0.06	0.42	0.13	0.79	0.40	0.11	0.14
K_2O	9.11	9.28	9.04	9.57	8.95	9.08	9.10	9.31
NiO	0.00	0.00	0.12	0.00	0.00	0.00	0.00	0.00
H_2O^+	3.25	3.17	3.33	2.93.	3.37	3.85	3.33.	4.11
F^-	0.10	0.50	0.08	0.15	0.19	0.29	0.09	0.13
Σ	98.88	99.08	99.30	98.86	99.53	100.89	99.87	99.84
fm	0.18	0.22	0.21	0.44	0.14	0.41	0.61	0.52
Crystal chemical coefficients								
Si	2.92	2.82	2.81	2.77	2.86	2.77	2.68	2.80
Al_{IV}	1.08	1.14	1.19	1.23	1.14	1.23	1.32	1.20
Ti_{IV}	0.00	0.04	0.00	0.00	0.00	0.00	0.00	0.00
Σ_{IV}	4.00	4.00	4.00	4.00	4.00	4.00	4.00	4.00
Ti	0.03	0.01	0.05	0.11	0.04	0.16	0.17	0.15
Al_{VI}	0.10	0.00	0.03	0.15	0.04	0.05	0.20	0.16
Cr	0.03	0.03	0.03	0.00	0.00	0.00	0.00	0.00
Fe^{3+}	0.06	0.18	0.09	0.05	0.08	0.04	0.08	0.16
Fe^{2+}	0.45	0.48	0.51	1.13	0.32	1.08	1.41	1.14
Mn	0.00	0.00	0.00	0.01	0.00	0.01	0.01	0.01
Mg	2.32	2.32	2.29	1.48	2.52	1.59	0.95	1.19
Ni	0.00	0.00	0.01	0.00	0.00	0.00	0.00	0.00
Σ_{VI}	2.99	3.02	3.01	2.93	2.92	2.93	2.82	2.81
Ca	0.01	0.01	0.00	0.01	0.00	0.01	0.07	0.01
Na	0.03	0.01	0.06	0.02	0.11	0.06	0.02	0.02
K	0.83	0.86	0.83	0.92	0.81	0.86	0.89	0.90
Σ_{XII}	0.87	0.88	0.89	0.95	0.92	0.93	0.98	0.93
Charge								
IV+VI	21.12	20.96	21.05	21.04	21.02	20.88	20.77	20.89

Note: FeO and Fe_2O_3 in the samples 26633; 410/225.0; 99/46.4 are determined by wet chemistry.
n.d. – not determined

synthetic phlogopite–annite series. But the micas from the borehole and surface form separate fields, the former characterized by lower values of *V* than the latter at similar *fm* values.

The degree of oxidation of Fe in both groups of micas is no more than 14−16% according to the Mössbauer data (Table 4). A discrepancy between results for the Fe oxidation state from Mössbauer, 'wet' chemistry and crystal chemistry calculations of microprobe data is seen. The portion of ferric Fe indicated by the Mössbauer data is 1.5−2 times lower than that suggested by other methods, but can be assumed to be more accurate. This indicates how important it is to determine the degree of oxidation of the Fe in minerals by the Mössbauer method.

Taking into account the Al-avoidance rule (Radoslovich, 1963) and experimental data for Al-bearing micas from NMR studies (Sanz *et al*., 1984), we assume that only the *M*1 sublattice

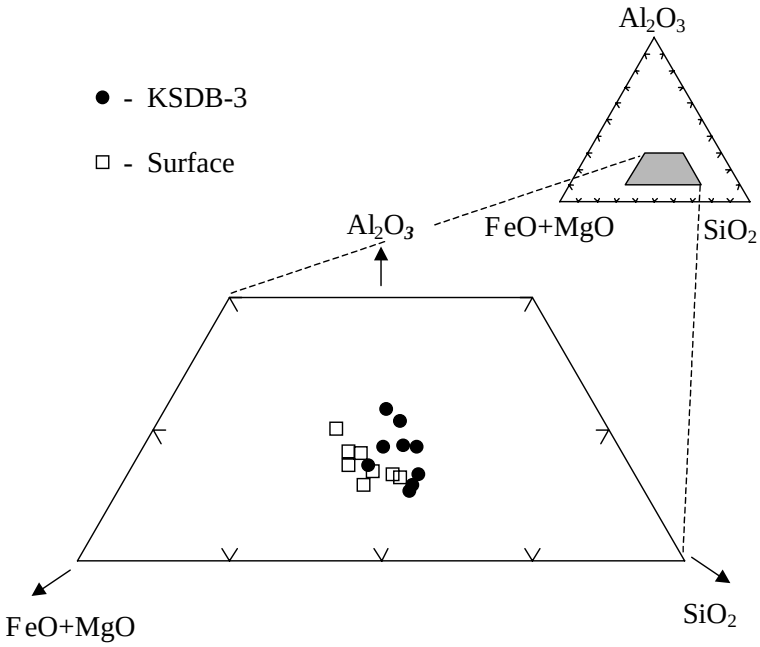

FIG. 1. (MgO+FeO)-Al_2O_3-SiO_2 diagram for the micas from amphibolites of the Archaean complex of KSDB-3 and their surface analogues.

contains vacancies, while trivalent cations Fe^{3+}, Al, Cr and Ti occupy the *M*2 sublattice (Table 5). The distribution of Fe has been refined from the Mössbauer data and is shown in Table 5 and in Fig. 3. It is obvious that in micas from the borehole, the distribution of Fe^{2+} between non-equivalent *M*1 and *M*2 octahedra is random, or the Fe^{2+} slightly prefers the *M*1 octahedra. In the

TABLE 3. Unit-cell parameters of micas.

Sample	*a* (Å)	*b* (Å)	*c* (Å)	β (°)	*V* (Å^3)
KSDB-3					
26633	5.327(1)	9.247(1)	10.271(1)	100.03(2)	498.1(2)
27053	5.338(1)	9.241(1)	10.248(1)	100.06(2)	497.7(2)
28248-g	5.313(1)	9.262(1)	10.272(1)	99.95(1)	497.9(2)
35899-2	5.320(1)	9.240(1)	10.252(1)	99.99(1)	496.3(2)
35967-4	5.320(1)	9.238(1)	10.250(1)	99.95(1)	496.2(2)
37483	5.329(1)	9.250(1)	10.245(1)	99.98(1)	497.4(2)
42749-2	5.326(1)	9.243(1)	10.244(1)	99.97(1)	496.7(1)
43452	5.335(1)	9.248(1)	10.239(1)	100.00(1)	497.5(2)
Surface					
410/135.0	5.325(2)	9.261(1)	10.273(3)	99.93(4)	498.9(3)
410/225.0	5.310(3)	9.244(1)	10.257(3)	99.83(4)	496.0(4)
130/40.7	5.334(2)	9.255(1)	10.256(2)	99.95(3)	498.6(3)
247/246.9	5.340(2)	9.259(2)	10.258(3)	100.02(4)	499.4(4)
9.10	5.342(2)	9.264(1)	10.242(3)	99.98(4)	499.2(3)
2757/71.0	5.337(2)	9.267(1)	10.251(3)	99.89(3)	499.5(3)

Note: Estimated standard deviations in parentheses refer to the last digit

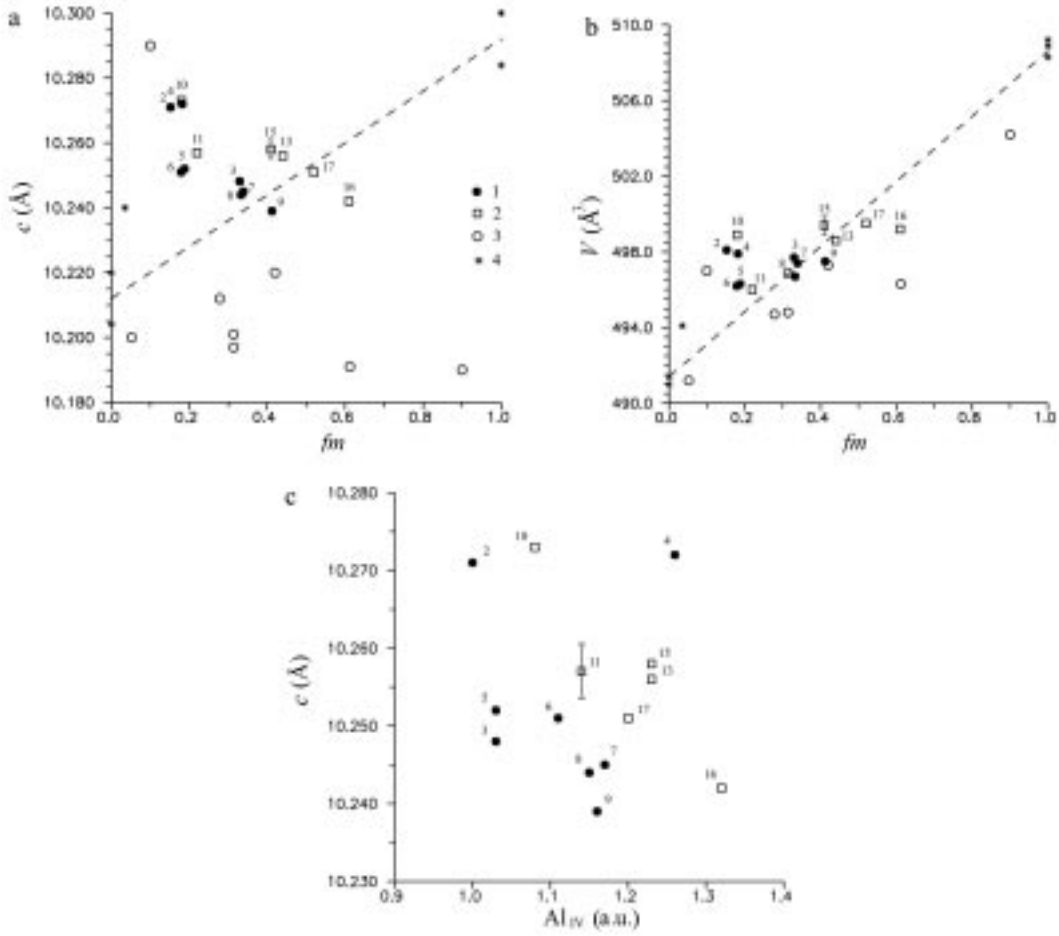

FIG. 2. Unit-cell parameter c (*a*) and unit-cell volume V (*b*) *vs*. *fm* in trioctahedral micas from the amphibolites of the Archaean complex probed in the borehole (1) and from surface Archaean rock analogues of the Allarechka block (2); (3) the micas from metamorphic rocks; and (4) micas from a synthetic phlogopite–annite series (Bailey, 1984). Note that micas of the two studied groups form several trends and in Fig. 1*a* the negative dependence of the c parameter on *fm* in contrast to the positive one for the micas from the synthetic phlogopite–annite series are shown.

micas from surface analogues, Fe^{2+} preferentially occupies *M*1 sites and Mg occupies *M*2 sites, and the cation distribution appears more ordered.

The IR spectra of all samples show OH^--stretching vibrations characteristic of triplets of divalent cations (N-bands), triplets of di- and trivalent cations (I-bands), as well as intense V bands indicative of clusters of two cations and a vacancy. Also observed are intense absorption W-bands due to stretching vibrations of H_2O molecules ($\nu_{H_2O^-}$) (Fig. 4). In general, such types of IR spectra are not typical of phlogopites and biotites of similar compositions from metamorphic and igneous rocks. Similar spectra, which reflect a high level of structural defects are observed mainly for micas from lamproites (Babushkina *et al*., 1997, 2000) and metasomatites.

Each of the N, I and V absorption bands are multiple and include the individual ν_{OH^-} bands that correspond to several triplets of the possible divalent (Mg, Fe, Mn, Ni) and trivalent (Al, Fe^{3+}, Cr, Ti^{3+}) cations. Moreover, the hydroxyl ion is coordinated by all cations of the hexagonal tetrahedral ring. The Si → Al substitution leads to different Si and Al combinations in these hexagonal rings (Ponomarev and Lapides, 1990) and, taking into consideration the Loewenstein rule (Loewenstein, 1954), four configurations are

TABLE 4. ^{57}Fe Mössbauer parameters (mm s^{-1}) of doublets and Fe_2O_3/ $FeO+Fe_2O_3$ (Mössbauer and wet chemistry data, %).

Sample	(1-1′)-Fe^{2+}_{2M2}				(2-2′)-Fe^{2+}_{M1}				(3-3′)-Fe^{3+}			$Fe_2O_3/FeO+Fe_2O_3$	
	QS	IS	HW	A (%)	QS	IS	HW	A (%)	QS	IS	HW	Mössbauer data	Wet chemistry
KSDB-3													
26524	2.704	1.210	0.310	67	2.320	1.185	0.301	33	0.689	0.378	0.672	11	14
27053	2.637	1.213	0.426	53	2.211	1.174	0.707	47	0.657	0.080	0.257	9	9
28248-g	2.664	1.221	0.306	63	2.408	1.119	0.465	37	0.845	0.435	0.521	12	35
35967-4	2.663	1.225	0.317	60	2.357	1.173	0.504	40	0.715	0.582	0.470	9	3
37483	2.673	1.211	0.321	50	2.284	1.212	0.410	50	0.951	0.614	0.343	8	7
42749-2	2.618	1.223	0.402	62	2.196	1.253	0.716	38	1.085	0.458	0.414	4	11
43452	2.536	1.246	0.465	68	2.456	1.032	0.440	32	0.472	0.519	0.432	11	20
Surface													
410/135.0	2.715	1.202	0.319	50	2.421	1.198	0.360	50	1.283	0.472	0.571	13	21
247/246.9	2.702	1.226	0.313	44	2.317	1.202	0.454	56	0.475	0.518	0.362	4	13
130/40.7	2.686	1.224	0.289	47	2.334	1.219	0.451	53	0.662	0.710	0.504	5	10
9,10	2.679	1.234	0.301	44	2.305	1.206	0.425	56	0.535	0.590	0.344	6	16
2757/71.0	2.715	1.212	0.275	35	2.342	1.212	0.476	65	0.986	0.588	0.795	13	13
1394/45.0	2.745	1.246	0.270	32	2.480	1.209	0.400	68	0.918	0.649	0.774	16	21

Note: in the sample 27053, cations of Fe^{3+} occupy tetrahedral positions.

TABLE 5. Distribution of cations and vacancies between non-equivalent positions by Mössbauer and IR methods.

Sample	*M*2			*M*1		
	X_{Mg}	X^{2+}_{Fe}	X^{3+}_{R}	X_{Mg}	X^{2+}_{Fe}	$X_{vac.}$
KSDB-3						
26524	0.61	0.24	0.15	0.64	0.23	0.13
26633	n.d	n.d	0.12	n.d	n.d	0.04
27053	0.56	0.20	0.24	0.55	0.36	0.09
28248-g	0.68	0.14	0.18	0.75	0.18	0.08
35899-2	n.d	n.d	0.14	n.d	n.d	0.06
35967-4	0.66	0.13	0.21	0.75	0.17	0.08
37483	0.58	0.20	0.22	0.52	0.41	0.07
42749-2	0.54	0.24	0.22	0.58	0.30	0.12
43452	0.54	0.33	0.14	0.60	0.31	0.09
Surface						
410/135.0	0.74	0.11	0.15	0.75	0.22	0.03
1394/45.0	0.82	0.08	0.10	0.57	0.35	0.08
130/40.7	0.56	0.26	0.18	0.29	0.60	0.11
247/246.9	0.62	0.24	0.14	0.27	0.60	0.13
9.10	0.46	0.31	0.24	0.05	0.79	0.16
2757/71.0	0.59	0.20	0.21	0.09	0.74	0.17

most likely: $6Si(H_0)$, $5SiAl(H_1)$, $4Si2Al(H_2)$ and $3Si3Al(H_3)$. The influence of each of these

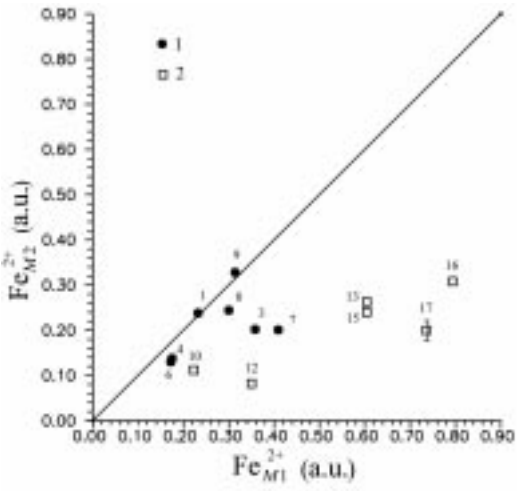

FIG. 3. The distribution of Fe^{2+} between non-equivalent *M*1 and *M*2 octahedral sites in the structure of micas from amphibolites of the Archaean complex probed in the borehole (1) and from analogous Archaean surface rocks of the Allarechka block (2). Note the random (or near-random) distribution of Fe^{2+} for micas from KSDB-3 (1) and increased preference of Fe^{2+} for *M*1 in micas from the surface rocks.

configurations on the hydroxyl ion is different and may lead to additional bands. Ponomarev and Lapides (1990) assigned the 3735 cm^{-1} band to a configuration at the octahedra and tetrahedra of 3Mg and H_0. The 3720 and 3710 cm^{-1} bands were assigned to the same 3Mg octahedral configuration and H_1 and H_2 ring configurations, respectively. But in some micas, substitutions such as Si → Al,Ti; Si → Al,Fe^{3+}; and Si → Al,Ti,Fe^{3+} may occur. These substitutions lead to additional configurations of tetrahedral cations: 4SiAlTi, 4SiAlFe^{3+}, 3SiAlTiFe^{3+}, which further complicate the IR spectra.

The assignment of IR bands between 3850 and 3000 cm^{-1} (Tables 6, 7) was carried out with reference to the compositions and data for the amount of Fe^{2+} and Fe^{3+} and the distribution of Fe^{3+} between tetrahedral and octahedral sites (from Mössbauer spectroscopy). In addition, the atomic weight and cation valence were taken into consideration. The variation in position of bands, corresponding to the same cation groups in samples with different overall composition, may be explained by the sensitivity of OH^- vibration to the occupation of the second and more distant coordination spheres. The assignment which best fitted the data for Fe^{2+}, Mg and R^{3+} content from wet chemistry and Mössbauer experiments was selected as the most likely.

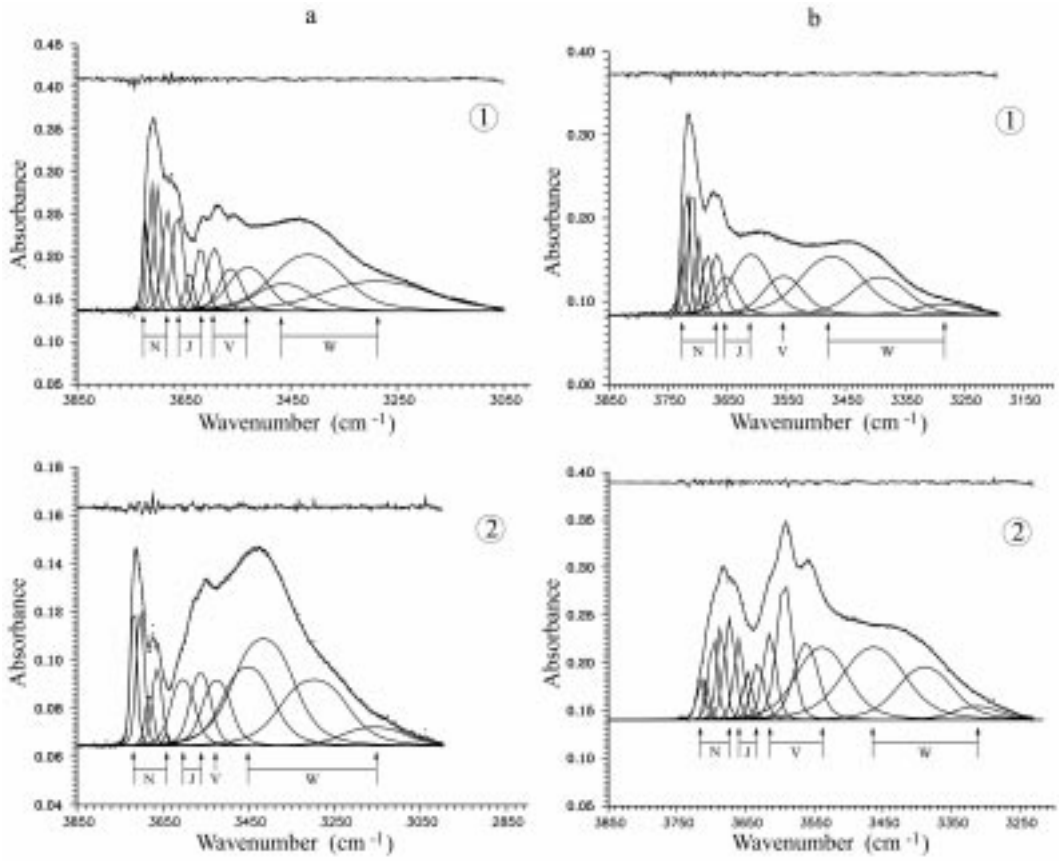

FIG. 4. The typical IR spectra of micas from amphibolites of the Archaean complex of KSDB-3 (a) (1 – sample 26524, 2 – sample 26633) and from surface analogues of the Allarechka block (b) (1 – sample 410/135.0, 2 – sample 2757/71.0) in the range 3800–3000 cm^{-1}.

The h_N:h_I:h_V = 1:0.56:0.10 coefficient relationship (Rousseaux *et al.*, 1972; Ponomarev and Lapides, 1988) was used in the N, I and V integral intensity absorption determination. It allowed us to determine the proportions of triple cation groups and to calculate the content (in a.u.) of octahedral cations Mg, Fe^{2+}, R^{3+} and V according to:

$$Mg = 3N_A + 2N_B + N_C + 2I_A + I_B + 2V_A + V_B + V_C$$
$$Fe = N_B + 2N_C + 3N_D + I_B + 2I_C + V_B + V_D$$
$$R^{3+} = I_A + I_B + I_C + V_C + V_D + 2V_E$$
$$Vac = V_A + V_B + V_C + V_D + V_E,$$

where N, I and V are the proportions of triple cation groups.

The discrepancies between the vacancy concentrations and octahedral cation contents calculated on the basis of proportions of triple cation groups and that obtained by Mössbauer and microprobe methods are shown in Tables 8 and 9. The mean square deviation is equal to 0.02–0.05 a.u., which confirms the correct assignment of the absorption bands.

Intense broad bands between 3495 and 3124 cm^{-1} are found in our spectra. Between two and six bands were fitted in this spectral region. Low-intensity water bending bands (δ_{H_2O}) occur between 1655 and 1620 cm^{-1}. We suppose that the bands at 3495–3317 cm^{-1} correspond to structural H_2O stretching, connected to the structure by weak hydrogen bonds, and the bands between 3312 and 3124 cm^{-1} correspond to the overtone of the water bending-vibration (Farmer, 1975). The relative amount of structural water we estimated as:

$$I_{H_2O}/I_{tot} = \Sigma W_{H_2O}/\Sigma(I_N + 0.56I_I + 0.1I_V) + \Sigma W_{H_2O}$$

where $\Sigma W_{H_2O} = I_{W1} + I_{W2} + I_{W3} + I_{W4}$: the total integral intensity of stretching vibrations of H_2O

TABLE 6. Assignment of hydroxyl-stretching bands (ν_{OH^-}) in the IR spectra of micas from KSDB - 3.

Cation configuration	Symbol	Position of ν_{OH^-} bands (cm^{-1})								
		26524	26633	27053	28248-g	35899-2	35967-4	37483	47249-2	43452
MgMgMg	N_A^2	3721	3718		3718	3717	3718	3717	3716	3715
MgMgMg	N_A^3	3711		3713	3709		3706			
MgMgMg	N_A^4		3702		3697	3705		3705	3704	3703
MgMgMg	N_A^5		3682							
$MgMgFe^{2+}$	N_B	3699		3698	3680	3689	3695	3693	3691	3689
$MgFe^{2+}Fe^{2+}$	N_C	3681	3664	3679		3672	3685	3676	3676	3674
$Fe^{2+}Fe^{2+}Fe^{2+}$	N_D		3643							3658
MgMgAl	I_A^1	3661	3604	3662	3666	3658	3672	3659	3662	3638
MgMgTi	I_A^2	3640		3640	3655		3658	3640	3650	3616
$MgMgFe^{3+}$	I_A^3					3624		3621		
$MgFe^{2+}Al$	I_B^1	3619		3618			3639	3607	3636	
$MgFe^{2+}Ti$	I_B^2		3562							
$MgFe^{2+}Cr$	I_B^3									3605
$Fe^{2+}Fe^{2+}Al$	I_C^1				3634			3592	3623	
MgAlV	V_C^1	3592	3525	3594	3618				3613	3594
MgTiV	V_C^2	3563		3572		3586		3584		3588
MgCrV	V_C^3				3593		3615	3562	3596	
$MgFe^{3+}V$	V_C^4				3565	3574	3590	3555	3570	3566
$Fe^{2+}AlV$	V_D^1				3521			3524	3521	
$Fe^{2+}CrV$	V_D^3	3529					3561			
$Fe^{2+}Fe^{3+}V$	V_D^4						3540			3515
$R^{3+}R^{3+}V$	V_E			3528(Al,Ti)						
H_2O	W_1	3463	3452	3471	3495	3473				
H_2O	W_2	3417	3446	3403	3414		3424	3430	3428	3433
H_2O	W_3					3392				
H_2O	W_4				3317			3337		3345
H_2O	W_5	3288	3298	3245		3287	3263		3295	3244
H_2O	W_6		3158						3124	

between 3495 and 3317 cm^{-1}. Such an evaluation is certainly only quasi-quantitative at best.

The dependence of the unit-cell parameter *c* on I_{H_2O}/I_{tot} (Fig. 5) confirms the incorporation of H_2O molecules into the mica structure. A negative correlation between the of amount of structural water and K content (0.66−0.86 a.u.) is observed in micas from the bore-hole section (Fig. 6). This suggests that the structural water molecules in these trioctahedral micas probably occupies the vacant interlayer cavities. Such a dependence is not observed for the micas from analogous surface rocks, in which the K content is a little larger (0.83−0.92 a.u.).

Discussion

The results of our study of the structure of trioctahedral ferromagnesium micas from the amphibolites of KSDB-3 Archaean complex and from analogous surface equivalents can be considered in several ways; firstly, in terms of implications for the crystal chemistry of trioctahedral ferromagnesium micas in general, and secondly, in terms of the structural properties of ferromagnesium micas from deep crustal zones.

One of the most important results is the refinement of the assignment of individual absorption bands for ν_{OH^-} in the N, I and V groups. Our micas are members of complex polycomponent solid solutions (see Table 2). In their structures, the octahedral sites are occupied by between four and seven different sorts of cations, additionally some of them may be vacant. The existence of 20−40 different combinations of triple groups, which are co-ordinated to the OH^- ion and which give rise to different corresponding ν_{OH^-} absorption bands, is theoretically possible. Moreover, additional complication of IR spectra may arise due to the influence and variety in occupation of the first, second and further co-ordination spheres. Using our combined approach

TABLE 7. Assignment of hydroxyl-stretching bands (ν_{OH^-}) in the IR spectra of surface micas.

Cation configuration	Symbol	Position of ν_{OH^-} bands (cm^{-1})							
		410/135	1394/45.0	130/40.7	247/246.9	9,10	2757/71.0	99/46.4	410/225.0
MgMgMg	N_A^1	3726						3726	3726
MgMgMg	N_A^2	3718	3721		3719		3715	3718	3719
MgMgMg	N_A^3	3709	3711	3708	3710		3706	3708	3712
MgMgMg	N_A^4	3698	3700	3700	3700	3699		3698	3705
MgMgMg	N_A^5		3682	3691					3700
$MgMgFe^{2+}$	N_B^1	3683	3663	3680	3689	3683	3697	3687	3694
$MgMgFe^{2+}$	N_B^2							3672	3674
$MgFe^{2+}Fe^{2+}$	N_C	3667	3644		3677	3665	3685		
$Fe^{2+}Fe^{2+}Fe^{2+}$	N_D			3667	3665	3645	3673		
MgMgAl	I_A^1	3652		3649	3656		3660	3646	
MgMgTi	I_A^2						3647		3654
$MgMgFe^{3+}$	I_A^3								3641
$MgFe^{2+}R^{3+}$	I_B	3610(Ti,Cr,Fe)	3632(Al,Fe)						
$MgFe^{2+}Al$	I_B^1					3612			
$MgFe^{2+}Ti$	I_B^2			3628	3641				
$MgFe^{2+}Fe^{3+}$	I_B^4						3632		
$Fe^{2+}Fe^{2+}Ti$	I_C^2				3620	3592			
MgMgV	V_A	3555		3602	3596	3578			
$MgFe^{2+}V$	V_B			3578	3564				
MgAlV	V_C^1						3615	3598	
MgTiV	V_C^2		3592	3546		3555	3593	3567	
MgCrV	V_C^3		3542						
$MgFe^{3+}V$	V_C^4					3533		3535	
$Fe^{2+}TiV$	V_D^2					3505			3534
$Fe^{2+}Fe^{3+}V$	V_D^4			3493	3538	3482	3539		
$R^{3+}R^{3+}V$	V_E						3526(Al,Ti)		
H_2O	W_1	3474	3462		3478	3450	3463		
H_2O	W_2		3415	3409	3408	3413		3424	3417
H_2O	W_3	3392			3346	3362	3388		
H_2O	W_5	3286				3305	3312	3276	3308
H_2O	W_6		3158						3124

we have achieved a self-consistent assignment of all ν_{OH^-} absorption bands for these natural micas. The refined assignment allows us to determine the contents of Mg, Fe^{2+} and R^{3+} cations as well as vacancies in the octahedral sheet to within a few hundredths of atomic units (see Table 8) on the basis of the integral intensity of ν_{OH^-} absorption bands and the Mössbauer data. For large contents of octahedral Al and Fe^{3+} (>0.1 a.u.) it is also possible to estimate the occupancies of these cations to within a few hundredths of atomic units (see Table 9). We therefore consider that our assignment of absorption bands for ν_{OH^-} vibrations is valid, and on this basis we can evaluate the octahedral sheet composition of these trioctahedral mica structures with relative accuracy.

The Mössbauer investigations presented here allow us to confirm experimentally the validity of the Radoslovich rule (Radoslovich, 1963) for trivalent cation ordering in the *M*2 site in trioctahedral micas. The dependence of quadrupole splitting of the doublet assigned to Fe^{2+} in the *M*1 site on the trivalent cation content in the octahedral sheet is very significant (Fig. 7). This dependence is negative and shows the decrease of local *M*1 site symmetry according to the Bancroft rule (Bancroft *et al*., 1967). The dependence of the QS of Fe^{2+} in the *M*2 site on the trivalent cation content in the octahedral sheet is also negative, but essentially weaker. This may be understood if we consider that the nearest neighbours for cations in *M*1 are six cations in the *M*2 site only and the nearest cation environment for cations in the *M*2 site is formed by three cations in *M*1 and three cations in *M*2. According to the Loewenstein rule (Loewenstein, 1954), the hexagonal ring cannot

TABLE 8. Comparison of wet chemistry (w/ch) and IR data (a.u.).

Sample	Mg			Fe^{2+}			R^{3+}			V		
	w/ch	IR	Δ	MS	IR	Δ	w/ch	IR	Δ	w/ch	IR	Δ
KSDB-3												
26524	1.86	1.88	−0.02	0.71	0.73	−0.02	0.30	0.30	0.00	0.14	0.13	+0.01
27053	1.66	1.65	+0.01	0.76	0.78	−0.02	0.42	0.49	−0.07	0.16	0.09	+0.07
26633	2.35	2.28	+0.07	0.42	0.44	−0.02	0.21	0.23	−0.02	0.02	0.04	−0.02
28248-g	2.20	2.11	+0.09	0.45	0.44	+0.01	0.38	0.36	+0.02	0.00	0.08	−0.08
35899-2	2.24	2.19	+0.05	0.39	0.46	-0.07	0.30	0.29	+0.01	0.07	0.06	0.01
35967-4	2.15	2.10	+0.05	0.43	0.40	+0.03	0.35	0.42	−0.07	0.06	0.08	−0.02
37483	1.71	1.70	+0.01	0.81	0.79	+0.02	0.39	0.44	−0.05	0.08	0.07	+0.01
42749-2	1.64	1.60	+0.04	0.79	0.85	−0.06	0.45	0.43	+0.02	0.12	0.12	0.00
43452	1.53	1.50	+0.03	0.97	0.98	−0.01	0.36	0.27	+0.09	0.14	0.09	+0.05
Surface												
410/135.0	2.32	2.30	+0.02	0.45	0.37	+0.08	0.22	0.30	−0.08	0.01	0.03	−0.02
1394/45.0	2.29	2.26	+0.03	0.51	0.46	+0.05	0.20	0.21	−0.01	0.00	0.08	−0.08
130/40.7	1.48	1.47	+0.01	1.13	1.06	+0.07	0.31	0.36	−0.05	0.07	0.11	−0.04
247/246.9	1.59	1.52	+0.07	1.08	1.06	+0.02	0.25	0.28	−0.3	0.07	0.12	−0.05
9,10	0.95	0.87	+0.08	1.41	1.49	−0.08	0.45	0.47	−0.02	0.18	0.16	+0.02
2757/71.0	1.20	1.25	−0.05	1.14	1.17	−0.03	0.47	0.42	+0.05	0.19	0.17	+0.02
σ			±0.05			±0.05			±0.05			±0.04

Note: Δ = w/ch – IR; σ – mean square deviation

TABLE 9. Comparison of trivalent cation content (a.u.) determined by wet chemistry (w/ch), Mössbauer and IR spectoscopy.

Sample	Al			Ti			Cr			Fe^{3+}		
	w/ch	IR	Δ_1	w/ch	IR	Δ_1	w/ch	IR	Δ_1	MS	IR	Δ_2
KSDB-3												
26524	0.14	0.14	0.00	0.05	0.06	−0.01	0.03	0.04	−0.01	0.08	0.08	0.00
26633	0.21	0.24	−0.04	0.04	0.03	+0.01						
28248-g	0.32	0.30	+0.02	–	–	–	0.01	0.02	−0.01	0.05	0.04	0.02
35899-2	0.10	0.14	−0.04	0.03	0.00	+0.03	0.04	0.00	+0.04	0.13	0.14	−0.01
35967-4	0.23	0.28	−0.05	0.04	0.07	−0.02	0.04	0.02	+0.02	0.04	0.05	−0.01
37483	0.20	0.24	−0.04	0.10	0.08	+0.02	0.02	0.02	0.00	0.07	0.10	−0.03
42749-2	0.36	0.32	+0.04	0.06	0.05	+0.01	0.00	0.03	−0.03	0.03	0.04	−0.01
43452	0.11	0.07	+0.04	0.12	0.12	0.00	0.02	0.01	+0.01	0.11	0.08	+0.03
Surface												
410/135.0	0.10	0.09	+0.01	0.03	0.07	−0.04	0.03	0.07	−0.05	0.06	0.07	−0.01
1394/45.0	0.03	0.03	0.00	0.05	0.05	0.00	0.03	0.03	0.00	0.09	0.09	0.00
130/40.7	0.14	0.18	−0.04	0.11	0.13	−0.02	–	–	–	0.05	0.05	0.00
247/246.9	0.05	0.042	+0.01	0.16	0.20	−0.04	–	–	–	0.04	0.05	−0.01
9,10	0.20	0.22	−0.02	0.17	0.19	−0.02	–	–	–	0.08	0.06	+0.02
2757/71.0	0.16	0.18	−0.02	0.15	0.16	−0.01	–	–	–	0.16	0.11	+0.04
99/46.4	0.04	0.13	−0.09	0.04	0.02	−0.02	–	–	–	0.08*	0.05	+0.03
410/225.0	–	–	–	0.01	0.02	−0.01	0.03	0.00	+0.03	0.18*	0.18	0.00
σ			±0.04			±0.02			±0.03			±0.02

Note: Δ_1 = w/ch – IR; Δ_2 = MS – IR; σ – standard deviation
* – wet chemical determination

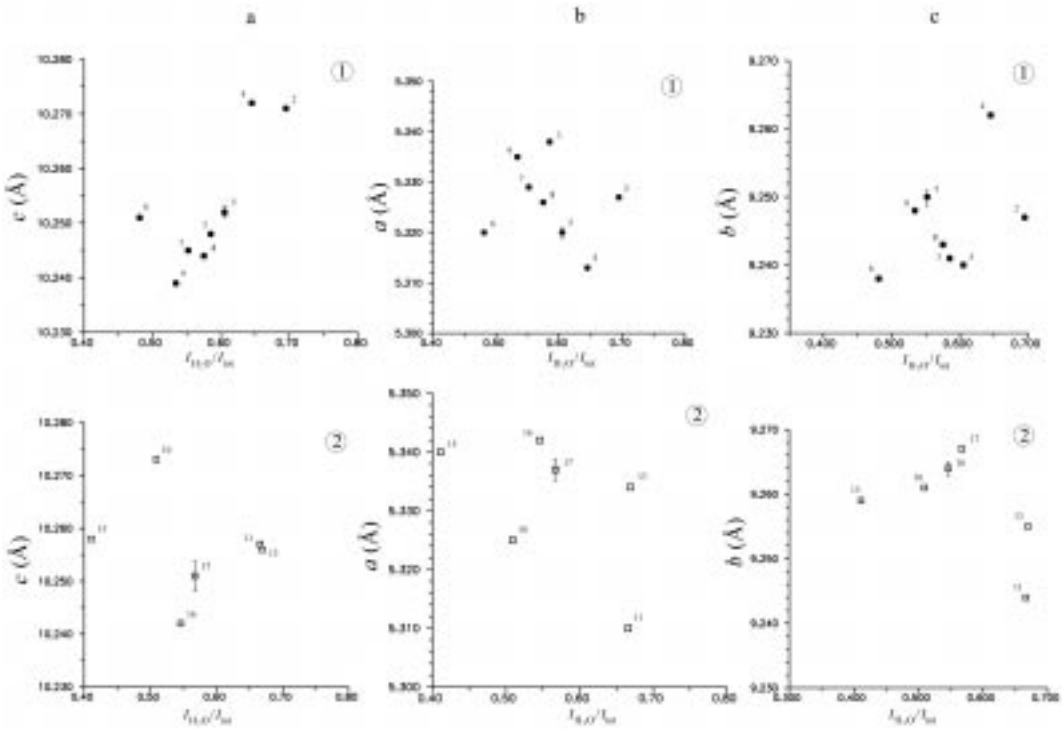

FIG. 5. Unit-cell parameters *a, b* and *c vs*. relative structural water in micas from: (1) amphibolites of the Archaean complex of KSDB-3; and (2) surface rocks of the Allarechka block.

contain more than three trivalent cations, but the probability of $4R^{2+}2R^{3+}$ or $3R^{2+}3R^{3+}$ combinations is small, because the trivalent cation content in the octahedra is <0.5 a.u. The presence of a trivalent cation in one of the *M*2 sites must reduce the symmetry of the cation environment for *M*1 as well as for *M*2 and will therefore lower the quadrupole splitting of Fe^{2+} in these sites. But if we suppose that trivalent cations may also occupy *M*1 sites, then these cations must only influence the symmetry of the *M*2 (not *M*1) environment. In this case the dependence of the QS of Fe^{2+} in *M*2

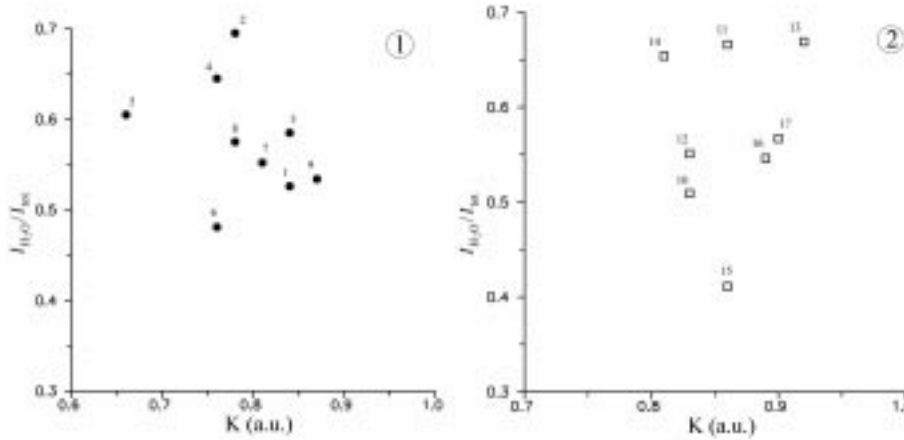

FIG. 6. Relative amounts of structural water *vs*. K content in micas (1) from amphibolites of the Archaean complex of KSDB-3; and (2) surface rocks of the Allarechka block.

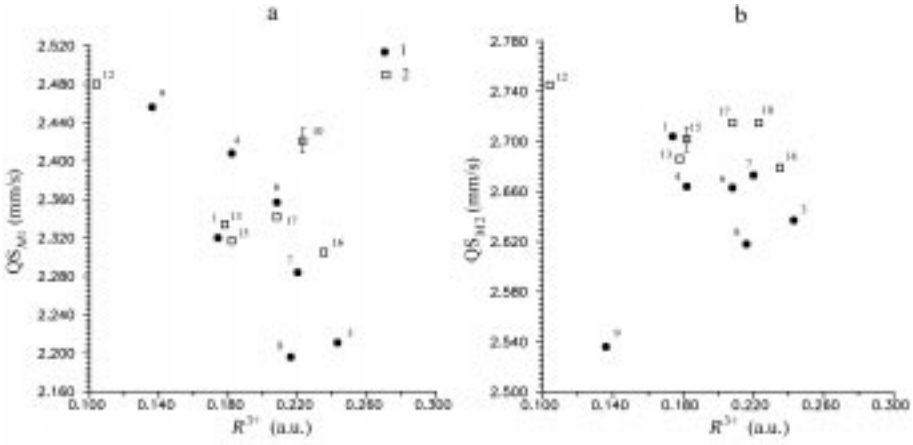

FIG. 7. The quadrupole splitting of Fe^{2+} in the *M*1 (*a*) and *M*2 (*b*) sites *vs*. trivalent cation content in micas (the symbols are the same as in Fig. 6). A negative dependence of QS_{FeM2} and QS_{FeM1} on R^{3+} content in *M*2 sites can be seen. This reflects the decreasing symmetry of the first cation co-ordination sphere; for $QS_{Fe^{2+}M2}$ this dependence is stronger.

on the trivalent cation content must be stronger than for Fe^{2+} in *M*1. In fact we observed the opposite, which demonstrates that trivalent cations preferentially occupy the *M*2 sites.

The only hydrous molecular species anticipated in the ideal structure of trioctahedral Fe-Mg micas are the OH^- ions discussed above. It is well known that most micas from metamorphic and igneous rocks only show OH^- ions. Our investigations indicate the additional presence of structural water in our micas. Connected to the sheet structure by hydrogen bonding, H_2O molecules probably occupy vacant interlayer sites. The entry of H_2O (r = 1.4 Å) molecules, which are larger than the alkaline cation usually occupying this site (r_{K^+} = 1.33 Å), leads to a deformation of the unit cell: it dilates along the *c* axis. The substitution of K^+ by neutral H_2O molecules is charge balanced by excess positive charge in the octahedral sheet and this is illustrated by the dependence of this structural water content on the total charge of cations in octahedral and tetrahedral sites (Fig. 8).

At present we do not know whether the presence of molecular water reflects the formation of mixed-layered compounds, which comprise vermiculite layers interleaving the host layers of the trioctahedral mica, or whether the water molecules are distributed throughout the structure randomly. The additional investigation of 001 reflections according to the experimental procedure of Dyakonov (1981) is needed to answer this question.

It seems that the occurrence of structural water in these micas explains the negative dependence of the *c* parameter on *fm* for samples from both rock groups, and the positive dependence for synthetic micas in the phlogopite–annite series. Moreover, many of the micas we have studied (especially those micas from the borehole) display a positive deviation from the straight line on the diagram of *V vs. fm*. Since these micas include those with trivalent cation (predominantly Al) occupancies at the octahedral layer of 0.2 to 0.5 a.u., negative deviation from the phlogopite–annite line would be anticipated. The unexpected positive deviation indicates that the structure of the micas from both the borehole as well as the

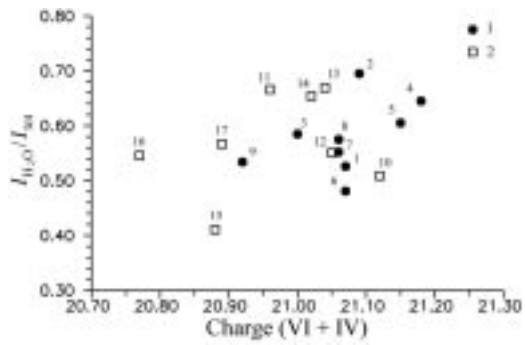

FIG. 8. Relationship between relative amounts of structural water and total positive charge of the tetrahedral and octahedral sheets. The symbols are the same as in Fig. 6.

surface, is somewhat 'spongy', even if the 'sponginess' of the surface micas is greater. For the micas from the borehole this is unexpected, taking into account their depth of formation (7900−11350 m).

In the micas under study, two types of 'defects' are highlighted; those connected with deviations from chemical stoichiometry and those associated with order-disorder. The compositional non-stoichiometry manifests itself in the existence of structural H_2O molecules, which probably occupy the vacant interlayer cavities, and in the existence of vacancies at the octahedral *M*1 sites. These defects are seen in the micas from the Archaean complex of the borehole as well as in their equivalents at the surface. The structural water content decreases very slightly with increasing depth for micas from the borehole (Fig. 9). It seems that the existence of structural water in micas of both groups reflects the special conditions of amphibolite metamorphism of the Archaean complex, with high partial pressure of water and a deficiency of alkalis.

Structural water preservation in the surface micas is probably best explained if the partial water pressure in the Archaean complex does not vary. Thus, the structural H_2O remains in the mica structure despite the total pressure and temperature decrease. It is not excluded, however, that some water may pass from interlayer cavities to interstitial sites. We note, for example, that surface micas plot in several fields with larger overall cell parameters than those of borehole micas with the same water content. Overall transport of cations is also needed to change the proportion of octahedral vacancies and form new micas. In a closed system, defects associated with non-stoichiometry cannot disappear simply upon changing pressure and temperature. Changes in partial water pressure as well as in the equilibrium distribution of Mg, Fe, Al cations and other components between micas and other mineral phases are also needed.

Differences in octahedral order-disorder are noted between micas from KSDB-3 (generally disordered) and in the equivalent surface micas (generally ordered). This is to be expected, taking into account the decreasing temperature of equilibration with decreasing depth. Experiments on Fe^{2+} order-octahedral disorder in natural trioctahedral micas were carried out by Babushkina (1993). The results showed two or three cation distribution steps with different activation energies. It seems that the temperature in the mid-crust, where the Archaean complex is situated (the temperature in borehole section was ~220°C), was sufficient to preserve the cation disorder of the mica structure. Using Babushkina's (1993) kinetic parameters for the micas with an Fe^{2+} content of 1.0 a.u. we estimate that it would take more than 250 years at this temperature to transform from complete disorder ($X_{Fe}^{M1} = X_{Fe}^{M2} = 0.33$) to complete order ($X_{Fe}^{M1} = 0.60$, $X_{Fe}^{M2} = 0.20$) state, which corresponds approximately to the degree of ordering in the surface micas. The elevation of the core during drilling took a few hours. As a result of such high-speed elevation from depth, the disorder in these micas is quenched in, and very low cation order is observed in all micas from the borehole. On the other hand, the very slow elevation experienced by micas from the Archaean complex, elevated due to erosion, at the surface allows equilibrium cation ordering to take place, and these samples are characterized by high degrees of cation order.

The results of the study of sulphides from KSDB-3 and the surface equivalents (Yakovlev and Neradovsky, 1998) are of great interest from the point of view of our mica order/disorder observations. Exsolution is observed in the surface sulphides but not in samples from the borehole. This demonstrates the differing conditions of equilibration in the two suites of samples, as well as confirming that those of the borehole are preserved as a result of quenching.

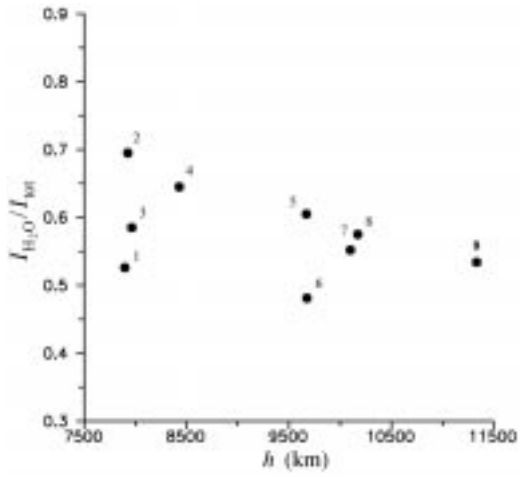

FIG. 9. Relative structural water content *vs*. mica depth in KSDB-3. The amount of structural water determined decreases with increasing depth.

Conclusions

This integrated study of chemical compositions (by wet chemistry and microprobe methods) and structural states (by XRD, Mössbauer and IR methods) of trioctahedral ferromagnesium micas from the amphibolites of KSDB-3 Archaean complex and from Archaean surface analogues provide important new results, both for the experimental procedure of such a study and the more general crystal chemistry of trioctahedral micas. We have also noted peculiar properties of the structure of micas from the deeper zones of the crust. In summary, this study has: (1) enabled the revision of the assignment of individual IR absorption bands for the hydroxyl ion (ν_{OH^-}), with revised assignments for the N, I and V bands; (2) demonstrated the possibility of determining the content of Mg, Fe^{2+}, R^{3+} cations and vacancies in the octahedral layer to within a few hundredths of atomic units on the basis of the integral intensity of IR absorbtion bands and Mössbauer data; (3) experimentally validated the Radoslovich rule (Radoslovich, 1963) concerning trivalent cation ordering in the *M*2 site; (4) demonstrated the existence of structural H_2O molecules, which seemingly occupy the cavities of interlayer replacing K^+; (5) shown a negative dependence of the *c* unit-cell parameter on *fm* for micas from KSDB-3 and their surface analogues, in contrast to the positive one observed for the end-members of synthetic phlogopite–annite series. It seems likely that this deviation is associated with the existence of structural H_2O in the interlayer; (6) established that, at the same *fm* values, these micas are characterized by the higher unit-cell volumes than the micas of the synthetic phlogopite–annite series. This indicates that the structure of these micas is expanded. For the micas from the borehole this is unexpected, taking into account their depth of formation (7900−11350 m) and the presence of up to 0.5 a.u. of trivalent cations in the tetrahedral layer; (7) established that the compositional non-stoichiometry of these micas is related to the presence of structural H_2O and of octahedral *M*1 vacancies, and that this occurs equally in samples from KSDB-3 and from surface rocks, perhaps reflecting the special conditions of amphibolite metamorphism in this Archaean complex (the increased water partial pressure and alkali deficiency); and (8) established that the cation order-disorder between the octahedral sites is different for micas from KSDB-3 (low cation order degree) and from analogous surface rocks (high cation order with Fe^{2+} showing preferential occupation of *M*1). This discrepancy is probably the result of different speeds of elevation of Archaean rocks from the deep zones due to drilling or erosion processes. This confirms our assumption regarding the quenching of the original structural features of the minerals (cation ordering and onset of exsolution) upon elevation of the core from the borehole.

Acknowledgements

This work was carried out in accordance with Project N 408 within International Geological Correlation Programme (IGCP) and was supported by RFFI N 99-05-65293, N 01-05-06082, N 00-05-72011.

References

Annersten, H., Devanarayanan, S., Häggström, L. and Wäppling, M. (1971) Mössbauer study of synthetic ferriphlogopite $KMg_3Fe^{3+}Si_3O_{10}(OH)_2$. *Physica Status Solidi* (b), **48**, 137.

Babushkina, M.S. (1993) Kinetics of the long range ordering of cations within natural biotite. *Zapiski Vserossiyskogo Mineralogicheskogo Obshchestva*, **1**, 37−47 (in Russian).

Babushkina, M.S. and Nikitina, L.P. (1985) Mössbauer study of cation distribution and the energetics of the biotite solid solution. *Proceedings of the International Conference on the Applied Mössbauer Effect*, London, 1812−1816.

Babushkina, M.S., Nikitina, L.P., Ovchinnikov, N.O. and Khiltova, E.Yu. (1989) The cation ordering, thermal expansion and thermodynamic properties of some Fe-bearing silicates. In*: Mineralogy. The reports of Soviet geologists in the XXVIII Geological Congress, Washington, July 1989*. Nauka (N.V. Sobolev, editor), 238 pp.

Babushkina, M.S., Nikitina, L.P., Ovchinnikov, N.O., Savva, E.V., Lukianova, L.I. and Genshaft, Yu.S. (1997) Composition and real structures of phlogopites from Kostomuksha lamproites. *Zapiski Vserossiyskogo Mineralogicheskogo Obshchestva*, **2**, 71−84 (in Russian).

Babushkina, M.S., Lepekhina, E.N., Nikitina, L.P., Ovchinnikov, N.O. and Lokhov, K.I. (2000) Structural distortion of micas from lamproites: Evidence from Mössbauer and IR spectroscopy. *Doklady Earth Sciences*, **371A**, 797−801 (translated from Russian).

Bailey, S.W. (1984) Crystal chemistry of the true micas. Pp. 13−60 in: *Micas* (S.W. Bailey, editor). Reviews

in Mineralogy, **13**, Mineralogical Society of America, Washington, D.C.

Bancroft, G.M. and Brown, J.S. (1975) A Mössbauer study of coexisting hornblendes and biotites: quantitative Fe^{3+}/Fe^{2+} ratios. *American Mineralogist*, **60**, 265–272.

Bancroft, G.M., Maddok, A.G. and Burns, R.G. (1967) Application of the Mössbauer effect to silicate mineralogy. I. Iron silicates of known structure. *Geochimca et Cosmochimica Acta*, **31**, 2219–2246.

Bohlen, S.R., Peacor, D.R. and Essene, E.J. (1980) Crystal chemistry of a metamorphic biotite and its significance in water barometry. *American Mineralogist*, **65**, 55–62.

Bosenick, A., Dove, M.T., Myers, E.R., Palin, E.J., Sainz-Diaz, C.I., Guiton, B.S., Warren, M.C., Craig, M.S. and Redfern, S.A.T. (2001) Computational methods for the study of energies of cation distributions: Applications to cation-ordering phase transitions and solid solutions. *Mineralogical Magazine*, **65**, 193–219.

Cruciani, G. and Zanazzi, P.F. (1994) Cation partitioning and substitution mechanisms in 1M phlogopite: A crystal chemical study. *American Mineralogist*, **79**, 289–301.

Cruciani, G., Zanazzi, P.F. and Quartieri, S. (1995) Tetrahedral ferric iron in phlogopite: XANES and Mössbauer compared to single-crystal X-ray data. *European Journal of Mineralogy*, **7**, 255–265.

Drits, V.A., Tepikin, V.E. and Aleksandrova, V.A. (1971) The creation of structural models of trioctahedral micas and ferrobiotite. Pp. 111–120 in: *Epigenesis and its Mineral Indicators*. Nauka, Moscow (in Russian).

Dyakonov, Yu.S. (1981) New data on species and identification of hydrobiotites. Pp. 39–46 in*: Crystal Chemistry of Minerals*. Nauka, Moscow (in Russian).

Dyar, M.D. (1987) A review of Mössbauer data on trioctahedral micas: evidence for tetrahedral Fe and cation ordering. *American Mineralogist*, **72**, 792–800.

Dyar, M.D. and Burns, R.G. (1986) Mössbauer spectral study of ferruginous one-layer trioctahedral micas. *American Mineralogist*, **71**, 955–988.

Evans, S. and Raftery, E. (1980) X-ray photoelectron studies of titanium in biotite and phlogopite. *Clay Minerals*, **3**, 209–217.

Farmer, V.C. (1974) The layer silicates. Pp. 331–363 in: *The Infrared Spectra of Minerals* (V.C. Farmer, editor). Monograph **4**, Mineralogical Society, London.

Farmer, V.C., Russell, J.D., McHardy, W.J. Newman, A.C.D., Ahlrichs, J.L. and Rimsaite, J.Y.H. (1971) Evidence of loss of protons and octahedral iron from oxidised biotites and vermiculites. *Mineralogical Magazine*, **38**, 121–137.

Henderson, C.M.B. and Foland, K.A. (1996) Ba- and Ti-rich primary biotite from the Brome alkaline igneous complex, Monteregian Hills, Quebec: Mechanisms of substitution. *Canadian Mineralogist*, **34**, 1241–52.

Ivanitskey, V.P., Matyash, I.V. and Rakovich, F.I. (1975) Effects of irradiation on the Mössbauer spectra of biotites. *Geochemistry International*, **12**, 151–157 (translated from *Geokhimiya*, **6**, 850–857).

Ivanitskey, V.P., Matyash, I.V., Plastinina, M.A., Sharkina, E.V., Pavlishin, V.I., Samsonov, V.A., Koval, V.B. and Taran, M.N. (1992) On the mechanism of transformation of phlogopite in hydrothermal solution (from experimental data) *Mineralogicheskiy Zhurnal*, **14**, 3–13 (in Russian).

Khristoforov, K.K., Nikitina, L.P., Kryjansky, L.M. and Ekimov, S.P. (1974) Kinetics of disordering of distribution of Fe^{2+} in orthopyroxene structures. *Transactions of the U.S.S.R. Academy of Sciences: Earth Science Section*, **214**, 165–167 (translated from *Doklady Akademii Nauk SSSR*, **214**, 909–912).

Lalonde, A.E. and Bernard, P. (1993) Composition and color of biotite from granites – 2 useful properties in the characterization of plutonic suites from the hepburn internal zone of wopmay orogen, north-west-territories. *The Canadian Mineralogist*, **31**, 203–17.

Lanev, V.S., Nalivkina, E.B., Vakhrusheva, V.V., Golenkina, E.A., Rusanov, M.S., Smirnov, Yu.P., Suslova, S.N., Duk, G.G., Koltzova, T.V., Maslenikov, V.A., Timopheev, B.V. and Zaslavskiy, V.G. (1984) The geological borehole section. Pp. 37–66 in: *Kola Superdeep* (V.A. Kozlovsky, editor). Nedra, Moscow (in Russian).

Loewenstein, W. (1954) The distribution of aluminium in the tetrahedra of silicates and aluminates. *American Mineralogist*, **39**, 92–96.

Loucks, R.R. (1991) The bound interlayer H_2O content of potassic white micas – muscovite-hydromuscovite-hydropyrophyllite solutions. *American Mineralogist*, **76**, 1563–1579.

Matveev, S.I., Novojilov, A.I., Kapustina, G.A. and Samoylovitch, M.I. (1981) Synthesis and some physical properties of fluorphlogopites with titanium admixture. Pp. 111–115 in*:* in*: Kola Superdeep Borehole. The Deep Construction Study of the Continental Core by Kola Superdeep Borehole Drilling* (V.A. Kozlovsky, editor). Nedra, Moscow (in Russian).

Mineeva, R.M. (1978) Relationship between Mössbauer spectra and defect structure in biotites from electric field gradient calculations. *Physics and Chemistry of Minerals*, **2**, 267–277.

Nalivkina, E.B. and Vinogradova, N.P. (1986) The rock forming minerals in the deep vertical section. Pp. 186–199 in: in*: Kola Superdeep Borehole. The Deep*

Construction Study of the Continental Core by Kola Superdeep Borehole Drilling (V.A. Kozlovsky, editor). Nedra, Moscow (in Russian).

Nalivkina, E.B., Lanev, V.S. and Vinogradova, N.P. (1984) Rocks and rock-forming minerals. Pp. 66–102 in: *Kola Superdeep Borehole. The Deep Construction Study of the Continental Core by Kola Superdeep Borehole Drilling* (V.A. Kozlovsky, editor). Nedra, Moscow (in Russian).

Nikitina, L.P. and Yakovleva, A.K. (1999) Crystal structure defects of minerals from Archean rocks in the section of Kola Superdeep borehole as the reflection of physical state of crystal substance in conditions of middle earth core. Pp. 88–93 in: *Rocks and Minerals at Great Depth and on the Surface: Subprojects.* KSC RAS, Apatity, Russia.

Ohta, T., Takeda, H. and Takeuchi, J. (1982) Mica polytypism: similarities in the crystal structures of coexisting 1M and $2M_1$ oxybiotite. *American Mineralogist*, **67**, 298–310.

Osherovich, E.Z. and Nikitina, L.P. (1975) Determination of content of elements in the octahedral positions in ferromagnesian micas by valence vibrations of OH^-. *Geochemistry International*, **5**, 71–76 (translated from *Geokchemiya*, **5**, 727–732).

Osherovich, E.Z., Nikitina, L.P. and Ekimov, S.P. (1978) Ferromagnesium micas. Pp. 127–136 in: *Cation Distributions and Thermodynamics of Ferromagnesium Solid Solutions of Silicates* (V.A. Glebovitsky, editor). Nauka, Moscow, (in Russian).

Pauling, L. (1960) *The Nature of the Chemical Bond*. Cornell University Press, Ithaca, USA, 548 pp.

Pavese, A., Ferraris, G., Pischedda, V. and Radaelli, P. (2000) Further study of the cation ordering in phengite 3*T* by neutron powder diffraction. *Mineralogical Magazine*, **64**, 11–18.

Pavlishin, V.I., Platonov, A.N., Polshin, E.V., Semenova, T.F. and Starova, G.L. (1978) The micas with iron in the tetradic coordination. *Zapiski Vserossiyskogo Mineralogicheskogo Obshchestva*, **107**, 165–180 (in Russian).

Ponomarev, B.G. and Lapides, I.L. (1988) The hydroxyl bond in micas – the analysis of cation distribution in tetrahedra and octahedra due to IR data. *Abstracts of VI All-Union isomorphism symposium, Zvenigorod*, 175, (in Russian).

Ponomarev, B.G. and Lapides, I.L. (1990) IR spectra of hydroxyl in sheet silicates: vacancies in biotites. *Mineralogicheskiy Zhurnal*, **1**, 78–82 (in Russian).

Radoslovich, E.W. (1963) The cell dimensions and symmetry of layer-lattice silicates. IV. Interatomic forces. *American Mineralogist*, **48**, 76–99.

Rancourt, D.G., Dang, M.-Z. and Lalonde, A.E. (1992) Mössbauer spectroscopy of tetrahedral Fe in trioctahedral micas. *American Mineralogist*, **77**, 34–43.

Rausell-Colom, J.A., Sanz, J., Fernández, M. and Serratosa, J.M. (1979) Distribution of octahedral ions in phlogopites and biotites. Pp. 27–36 in: *Developments in Sedimentology*, **27** (M.M. Mortland and V.C. Farmer, editors). Elsevier, Amsterdam.

Rousseaux, J.M., Gomes-Laverde, C., Nathan, Y. and Rouxhet, P.G. (1972) Correlations between the hydroxyl stretching band and the chemical composition of trioctahedral micas. Pp. 89–98 in: *Proceedings of the International Clay Conference Madrid* (J.M. Serratosa, editor). Division de Ciencias CSIC, Madrid.

Sanz, J. and Stone, W.E.E. (1977) NMR study of micas. I. Distribution of Fe^{2+} ions on the octahedral sites. *Journal of Chemical Physics*, **67**, 3739–3745.

Sanz, J. and Stone, W.E.E. (1979) NMR study of micas, II. Distribution of Fe^{2+}, F^- and OH^- in the octahedral sheet of phlogopites. *American Mineralogist*, **64**, 119–126.

Sanz, J. and Stone, W.E.E. (1983) NMR applied to minerals: IV. Local order in the octahedral sheet of micas: Fe-F avoidance. *Clay Minerals*, **18**, 187–192.

Sanz, J., Meyers, J., Vielvoye, L. and Stone, W.E.E. (1978) The location and content of iron in natural biotites and phlogopites: a comparison of several methods. *Clay Minerals*, **13**, 45–52.

Sanz, J., Gonzales-Carreno, T. and Gancedo, K. (1983) On dehydroxylation mechanisms of a biotite in vacuo. *Physics and Chemistry of Minerals*, **9**, 14–18.

Sanz, J., De la Calle, C. and Stone, W.E.E. (1984) NMR applied to minerals. V. The localization of vacancies in the octahedral sheet of aluminous biotites. *Physics and Chemistry of Minerals*, **11**, 235–246.

Saxena, S.K., Tazzoli, V. and Domeneghetti, M.C. (1987) Kinetics of Fe-Mg distribution in aluminous orthopyroxenes. *Physics and Chemistry of Minerals*, **15**, 140–147.

Semenova, T.F., Rozdestvenskaya, I.V. and Frank-Kamenetsky, V.A. (1977) The structure refinement of hydroxyl-phlogopite in connection with isomorphism in phlogopite–tephroite series. Pp. 101–109 in: *The Question of Isomorphism and Genesis of Mineral Individuals and Complexes*. Elista, Russia (in Russian).

Semenova, T.F., Rozdestvenskaya, I.V., Frank-Kamenetsky, V.A. and Pavlishin, V.I. (1983) Crystal structure of tetraferriflogopite and tetraferribiotite. *Mineralogicheskiy Zhurnal*, **5**, 41–49 (in Russian).

Skogby, H. (1987) Kinetics of intracrystalline order-disorder reactions in tremolite. *Physics and Chemistry of Minerals*, **14**, 521–526.

Smirnov, Yu.P., Lanev, V.S. and Guberman, D.M. (1991) The geological construction of the section. Pp. 14–12 in: *The Archean Complex in KSDB-3*

section (F.P. Mitrofanov, editor). KSC RAS, Apatity, Russia (in Russian).

Takeda, H. and Ross, M. (1975) Mica polytypism: dissimilarities in the crystal structures of coexisting 1M and $2M_1$ biotite. *American Mineralogist*, **60**, 1030–1040.

Tischendorf, G., Forster, H.J. and Gottesmann, B. (2001) Minor- and trace-element composition of trioctahedral micas: A review. *Mineralogical Magazine*, **65**, 249–76.

Vedder, W. (1964) Correlations between infrared spectrum and chemical composition of mica *American Mineralogist*, **49**, 736–768.

Virgo, A. and Hafner, S.S. (1969) Fe^{2+}, Mg order-disorder in heated orthopyroxenes. Mineralogical Society of America, *Special paper* **2**, 67–81.

Wilkins, R.W.T. (1967) The hydroxyl stretching region of the biotite mica spectrum. *Mineralogical Magazine*, **36**, 325–333.

Yakovlev, Yu.N. and Yakovleva, A.K. (1974) *The Mineralogy and Geochemistry of Copper-nickel ores*. Nauka, Moscow, 330 pp. (in Russian).

Yakovlev, Yu.N. and Yakovleva, A.K. (2000) Amphibolites of the Kola Superdeep Archean section. Pp. 77–82 in: *The Results of the Study of the Deep Substance and Pysical Processes in the Kola Superdeep Borehole Section down to a Depth of 12261 m* (Project 408). Poligraph, Apatity, Russia.

Yakovlev, Yu.N., Yakovleva, A.K. and Neradovsky, Yu.N. (1981) *The Mineralogy of Copper-nickel Deposits of Kola Peninsula* (G.I. Gorbunov, editor). Nauka, Moscow, 352 pp. (in Russian).

Yakovleva, A.K., Smirnov, Yu.P. and Yakovlev, Yu.N. (1991) Amphibolites rocks. Pp. 30–42 in: *The Archean complex in KSDB-3 section* (F.P. Mitrofanov, editor). KSC RAS, Apatity, Russia (in Russian).

Yuakovleva, A.K. (1991) The melanocratic minerals. Pp. 67–117 in: *The Archean complex in KSDB-3 section* (F.P. Mitrofanov, editor). KSC RAS, Apatity, Russia (in Russian).

Zagorodniy, V.G. and Radchenko, A.T. (1978) The principles and main features of tectonic zoning of north-eastern part of Baltic shield. Pp. 3–12 in: *Tectonic and Deep Texture of North-eastern part of Baltic Shield*. KF AN USSR, Apatity, Russia (in Russian).

[*Manuscript received 30 June 2001: revised 31 May 2002*]